

Protonated Ethane. A Theoretical Investigation of C₂H₇⁺ Structures and Energies

José Walkimar de M. Carneiro,^{†‡} Paul von R. Schleyer,^{*‡} Martin Saunders,[§] Richard Remington,[⊥] Henry F. Schaefer III,[⊥] Arvi Rauk,^{||} and Theodore S. Sorensen^{||}

Contribution from the Computer Chemistry Center, Institut für Organische Chemie der Friedrich-Alexander Universität Erlangen-Nürnberg, Henkestrasse 42, D-91054 Erlangen, Germany, Department of Chemistry, Yale University, New Haven, Connecticut 06520, Center for Computational Quantum Chemistry, University of Georgia, Athens, Georgia 30602, and Department of Chemistry, University of Calgary, Calgary, Alberta, Canada T2N 1N4

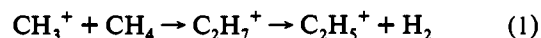
Received March 24, 1993. Revised Manuscript Received October 28, 1993*

Abstract: The C₂H₇⁺ potential energy surface was characterized by high-level *ab initio* calculations. The effects of electron correlation on geometries and relative energies are substantial. At MP4(SDTQ)/6-311G**//MP2(full)/6-31G**, the global minimum is the C–C protonated structure **1**, 4.4 kcal/mol (corrected to 298 K) more stable than the C–H protonated form **3**. The proton affinity of ethane to give **1** (142.5 kcal/mol) is 12.5 kcal/mol greater than that of methane (130 kcal/mol). Methane adds to the methyl cation, leading to **1** without activation energy. Barriers for intramolecular hydrogen interchange are lower than the dissociation energy into the ethyl cation and hydrogen, consistent with the experimental observation that deuterium scrambling is faster than dissociation. C₂H₇⁺ loses H₂ by 1,1-elimination in an endothermic (10.6 kcal/mol) process. Three frequencies deduced experimentally for C₂H₇⁺ correspond to those computed for **1**, but neither **2**, the H₂-rotated C–H protonated form, nor **3** can explain the other set of experimental spectral data. Complexes between H₂ and bridged C₂H₅⁺ were located, but they are too weakly bonded to be detected experimentally.

Protonated alkanes are important intermediates in saturated hydrocarbon transformations.¹ These nonclassical carbonium ions usually are characterized by three-center, two-electron bonded structures having pentacoordinated carbon atoms and bridging hydrogens.^{1–3} The simplest alkonium ion, CH₅⁺, was first reported by Tal'roze and Lyubimova.⁴ Higher homologues (C_nH_{2n+3}⁺) also were detected later in high-pressure mass spectrometry experiments.⁵ These carbonium ions are formed in the gas phase by ion–molecule reactions involving primary ions and neutral hydrocarbons or through simple proton-transfer reactions between the methonium ion and higher alkanes.

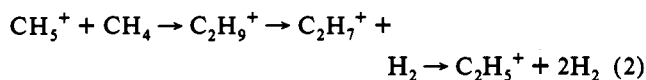
As part of an extensive investigation of electrophilic reactions of single bonds, Olah et al. examined the behavior of simple alkonium ions.^{1a,b,6} While these species are not directly observable in superacid solution, methane and ethane undergo hydrogen exchange and polycondensation to produce tertiary alkyl cations. This alkane condensation is assumed to start with reversible methane protonation leading to the methonium ion, CH₅⁺. This

species is believed to lose a hydrogen molecule to form the highly reactive (but not directly observable) methyl cation. CH₃⁺ reacts with excess methane to form the ethonium ion, C₂H₇⁺, which in turn decomposes into H₂ and the ethyl cation (eq 1). The process of building up higher carbocations continues with the reaction of C₂H₅⁺ with methane.



Protonated ethane, C₂H₇⁺, is the key intermediate in this mechanism. Olah and co-workers proposed that protolytic cleavage reactions and hydrogen–deuterium exchange as well as polycondensation of alkanes in superacid systems take place through protolysis of C–C or C–H bonds. These single bonds act as σ -electron donors; protonation leads to transition states or intermediates characterized by three-center bonded pentacoordinated carbonium ions.^{6b} Olah and co-workers were the first to note that various protonation sites are possible for ethane and the higher alkanes.^{6b} Ethane itself prefers C–C over C–H bond protonation.^{6c} An essentially symmetrical H-bridged structure was suggested to be the preferred form of the ethonium ion, C₂H₇⁺.

As the loss of H₂ from CH₅⁺ is quite endothermic, an alternative mechanism which circumvents the formation of CH₃⁺ in a discrete step is conceivable. The H₂ loss from CH₅⁺ and the reaction with CH₄ might be concerted (eq 2). Indeed, not only C₂H₅⁺ but also



[†] Permanent address: UFF-Instituto de Química, Department of Inorganic Chemistry, Outeiro de Sao Joao Batista-3^o Andar, 24020-Niteroi-RJ, Brazil.

[‡] Universität Erlangen-Nürnberg.

[§] Yale University.

[⊥] University of Georgia.

^{||} University of Calgary.

* Abstract published in *Advance ACS Abstracts*, February 1, 1994.

(1) (a) Olah, G. A.; Prakash, G. K. S.; Williams, R. E.; Field, L. D.; Wade, K. *Hypercarbon Chemistry*; Wiley-Interscience: New York, 1987; p 148f. (b) Olah, G. A.; Prakash, G. K. S.; Sommer, J. *Superacids*; Wiley-Interscience: New York, 1985; p 125f. (c) Vogel, P. *Carbocation Chemistry*; Elsevier: Amsterdam, 1985; pp 63, 103, 167.

(2) For a discussion of three-center bonded systems see ref 1a, p 13f, ref 1b, and ref 3.

(3) Olah, G. *J. Am. Chem. Soc.* **1972**, *94*, 808–820.

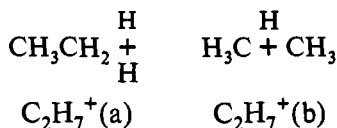
(4) Tal'roze, V. L.; Lyubimova, A. K. *Dokl. Akad. Nauk SSSR* **1952**, *86*, 909–912; *Chem. Abstr.* **1953**, *47*, 2590g.

(5) (a) Wexler, S.; Jesse, N. *J. Am. Chem. Soc.* **1962**, *84*, 3425–3432. (b) Field, F. H.; Franklin, J. L.; Munson, M. S. B. *J. Am. Chem. Soc.* **1963**, *85*, 3575–3583. (c) Field, F. H.; Munson, M. S. B. *J. Am. Chem. Soc.* **1965**, *87*, 3289–3294. (d) Munson, M. S. B.; Field, F. H. *J. Am. Chem. Soc.* **1965**, *87*, 3294–3299 and references cited therein. (e) Aquilanti, V.; Volpi, G. G. *J. Chem. Phys.* **1966**, *44*, 2307–2313. (f) For a summary, see: Field, F. H. *Acc. Chem. Res.* **1968**, *1*, 42–49.

(6) (a) Olah, G. A.; Lukas, J. *J. Am. Chem. Soc.* **1967**, *89*, 2227–2228. (b) Olah, G. A.; Klopman, G.; Schlosberg, R. H. *J. Am. Chem. Soc.* **1969**, *91*, 3261–3268. (c) Olah, G. A.; Halpern, Y.; Shen, J.; Mo, Y. K. *J. Am. Chem. Soc.* **1971**, *93*, 1251–1256. (d) Olah, G. A.; Olah, J. A. *J. Am. Chem. Soc.* **1971**, *93*, 1256–1259. (e) Olah, G. A.; Mo, Y. K.; Olah, J. A. *J. Am. Chem. Soc.* **1973**, *95*, 4939–4951. (f) Olah, G. A.; DeMember, J. R.; Shen, J. *J. Am. Chem. Soc.* **1973**, *95*, 4952–4956. (g) Olah, G. A.; Halpern, Y.; Shen, J.; Mo, Y. K. *J. Am. Chem. Soc.* **1973**, *95*, 4960–4970.

higher $\text{CH}_5^+(\text{CH}_4)_n$ complexes are observed in the gas phase.^{7b,8} Although several authors have studied proton-deuterium exchange and randomization in the C_2H_7^+ system,⁹ Saunders, Cross, et al.¹⁰ were the first to carry out experiments designed to gain more specific structural information. Deuterium-labeled methane and methyl cations were employed to investigate the scrambling and dissociation mechanisms. After decomposition, the end products are the ethyl cation and a hydrogen molecule (eq 1). On the assumptions that the extra proton is associated with one but not both of the carbon atoms (i.e., $\text{H}_3\text{C}-\text{CH}_4^+$) and that the decomposition of C_2H_7^+ always takes place from the pentacoordinated carbon atom by 1,1-elimination, a kinetic model was proposed to explain the H-scrambling observed. This occurs through an C_2H_7^+ intermediate which is short-lived but sufficiently well-defined to permit deuterium scrambling before decomposition occurs.¹⁰

Starting in 1975, Kebarle et al. reported a quantitative investigation of several protonated alkanes using high-pressure ion source mass spectrometry.^{7,8} For example, French and Kebarle's direct measurement of the decomposition of C_2H_7^+ into C_2H_5^+ and H_2 gave $E = 10.5 \pm 2.0$ kcal/mol.^{7c} By studying the rates and equilibria for addition of H_2 to C_2H_5^+ , Hiraoka and Kebarle observed that two different C_2H_7^+ isomers were produced, depending on temperature.⁸ At very low temperatures (-130 °C to -160 °C), H_2 added to C_2H_5^+ to form a $\text{C}_2\text{H}_7^+(\text{a})$ species in an exothermic third-body-dependent reaction without activation energy. At temperatures above -130 °C, the $\text{C}_2\text{H}_7^+(\text{a})$ species started to rearrange, and between -100 °C and $+40$ °C, a new and more stable $\text{C}_2\text{H}_7^+(\text{b})$ species was formed. At temperatures between 40 °C and 200 °C, the $\text{C}_2\text{H}_7^+(\text{b})$ ion decomposed back into $\text{C}_2\text{H}_5^+ + \text{H}_2$. The $\text{C}_2\text{H}_7^+(\text{a})$ isomer was identified as a C-H protonated ethane, while the more stable $\text{C}_2\text{H}_7^+(\text{b})$ was considered to be a C-C protonated form.



The activation energy for conversion of $\text{C}_2\text{H}_5^+ + \text{H}_2$ into $\text{C}_2\text{H}_7^+(\text{b})$ was estimated to be 1.2 kcal/mol via kinetic measurements in the -100 °C to $+40$ °C range. Measurements of the temperature dependence of the equilibrium $\text{C}_2\text{H}_5^+ + \text{H}_2 \rightleftharpoons \text{C}_2\text{H}_7^+$ gave $\Delta H_a = -4.0$ kcal/mol and $\Delta H_b = -11.8$ kcal/mol for the low- and high-temperature species, respectively. These data imply that the activation energy for loss of H_2 from $\text{C}_2\text{H}_7^+(\text{b})$ should be $1.2 + 11.8$, 1.8, or 13.0, kcal/mol. This was larger than the directly-measured 10.5 kcal/mol reported earlier,^{7c} but both values were considered to be in agreement, considering the "expected error limit". The energy barrier for the isomerization of $\text{C}_2\text{H}_7^+(\text{a})$ into $\text{C}_2\text{H}_7^+(\text{b})$ was deduced to be 5.2 kcal/mol.⁸ Kebarle's experimental results are summarized in Figure 1. This figure is also based on thermochemical data for the other species, CH_4 , CH_3^+ , and C_2H_5^+ .

Saunders and Cross's findings require that deuterium scrambling, starting with labeled CH_3^+ and CH_4 , occurs before dissociation into H_2 and C_2H_5^+ takes place. This implies that the

(7) (a) Hiraoka, K.; Kebarle, P. *J. Chem. Phys.* **1975**, *63*, 394–397. (b) Hiraoka, K.; Kebarle, P. *J. Am. Chem. Soc.* **1975**, *97*, 4179–4183. (c) French, M.; Kebarle, P. *Can. J. Chem.* **1975**, *53*, 2268–2274. (d) Hiraoka, K.; Kebarle, P. *Can. J. Chem.* **1975**, *53*, 970–972.

(8) (a) Hiraoka, K.; Kebarle, P. *J. Am. Chem. Soc.* **1976**, *98*, 6119–6125. (b) Hiraoka, K.; Kebarle, P. *Adv. Mass Spectrom.* **1978**, *7b*, 1408–1418.

(9) (a) Huntress, W. T., Jr. *J. Chem. Phys.* **1972**, *56*, 5111–5120. (b) Herman, Z.; Hierl, P.; Lee, A.; Wolfgang, R. *J. Chem. Phys.* **1969**, *51*, 454–455. (c) Ding, A.; Henglein, A.; Lacmann, K. *Z. Naturforsch.* **1968**, *23A*, 780–781. (d) Abramson, F. P.; Futrell, J. H. *J. Chem. Phys.* **1966**, *45*, 1925–1931. (e) Bohme, D. K.; Fennelly, P.; Hemsworth, R. S.; Schiff, H. I. *J. Am. Chem. Soc.* **1973**, *95*, 7512–7513.

(10) Weiner, J.; Smith, G. P. K.; Saunders, M.; Cross, R. J., Jr. *J. Am. Chem. Soc.* **1973**, *95*, 4115–4120. Cf. Heck, A. J. R.; deKoning, L. J.; Nibbering, N. M. M. *Int. J. Mass. Spectrom. Ion Processes* **1992**, *117*, 145.

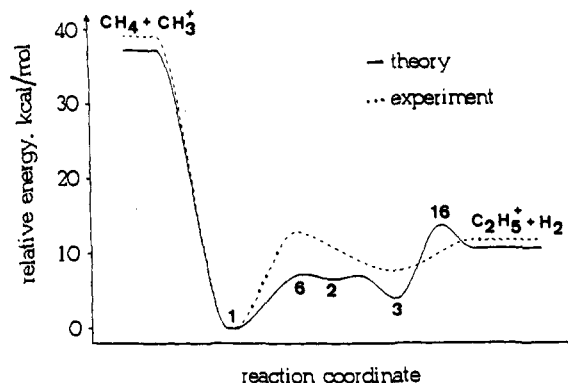


Figure 1. Potential energy diagram for reaction 1. Dashed curve is based on data from ref 8. The full curve is based on data from this work.

barrier to scrambling is lower than the dissociation energy.¹⁰ Kebarle's results indicate the C-H protonated form ($\text{C}_2\text{H}_7^+(\text{a})$) to be formed first from C_2H_5^+ and H_2 ,⁸ $\text{C}_2\text{H}_7^+(\text{a})$ is also the species from which loss of H_2 is believed to occur. Scrambling may occur prior to conversion into $\text{C}_2\text{H}_7^+(\text{b})$, but this process, according to Kebarle's newer data, requires a higher activation energy than decomposition into C_2H_5^+ and H_2 . In the crossed-beam experiment, the reactant species have excess energy when they combine and cannot relax unless collision with a third body takes place. Hence, more than sufficient energy is available for rearrangements. This can be followed by a further step leading, e.g., back to the original chemical structure with rearranged isotopes.

More recently, Lee et al. were able to deduce the infrared spectrum of the C_2H_7^+ ion.¹¹ They observed two sets of spectral features which were attributed to two different kinds of C_2H_7^+ structures. By analyzing the dependence of band intensities on the backing pressure and on the mixing ratio of hydrogen to ethane, these authors assigned the experimentally observed frequencies to the vibrational modes in the C-C and C-H protonated structures. In particular, they assigned a frequency at 3964 cm^{-1} to the H-H stretching vibration in a loose $\text{C}_2\text{H}_5^+\cdot\text{H}_2$ complex.¹¹ This frequency was compared with those of other H_2 complexes but did not receive support from the (privately communicated)¹¹ *ab initio* computed spectra of Dupuis.

As all the experiments described above give only general information about structure, a complementary theoretical examination is indispensable. This is particularly so for such a system whose unusual characteristics may determine its behavior. The structure of CH_5^+ has been investigated extensively by theoretical methods,^{12–15} but the potential energy surface of protonated ethane, C_2H_7^+ , is significantly more complicated and has not been elucidated fully.¹⁶ Earlier theoretical studies on C_2H_7^+ all agreed that the C-C protonated species is more stable

(11) Yeh, L. I.; Price, J. M.; Lee, Y. T. *J. Am. Chem. Soc.* **1989**, *111*, 5597–5604.

(12) (a) Lathan, W. A.; Hehre, W. J.; Pople, J. A. *J. Am. Chem. Soc.* **1971**, *93*, 808–815. (b) Lathan, W. A.; Lehre, W. J.; Curtiss, L. A.; Pople, J. A. *J. Am. Chem. Soc.* **1971**, *93*, 6377–6387. (c) Hariharan, P. C.; Lathan, W. A.; Pople, J. A. *Chem. Phys. Lett.* **1972**, *14*, 385–388. (d) Schleyer, P. v. R.; Apeloig, Y.; Arad, D.; Luke, B. T.; Pople, J. A. *Chem. Phys. Lett.* **1983**, *95*, 477.

(13) (a) Raghavachari, K.; Whiteside, R. A.; Pople, J. A.; Schleyer, P. v. R. *J. Am. Chem. Soc.* **1981**, *103*, 5649–5657. (b) Schleyer, P. v. R.; Carneiro, J. W. de M. *J. Comput. Chem.* **1992**, *13*, 997–1003. (c) Schreiner, P. R.; Kim, S.-J.; Schleyer, P. v. R.; Schaefer, H. F., III. *J. Chem. Phys.* **1993**, *99*, 3716–3720.

(14) (a) Klopper, W.; Kutzelnigg, W. *J. Phys. Chem.* **1990**, *94*, 5625–5630. (b) Dyzmowski, V.; Staemmler, V.; Kutzelnigg, W. *Chem. Phys. Lett.* **1970**, *5*, 361–366. (c) Kollmar, H.; Smith, H. O. *Chem. Phys. Lett.* **1970**, *5*, 7–9. (d) Gamba, A.; Morosi, G.; Simonetta, M. *Chem. Phys. Lett.* **1969**, *3*, 20–21.

(15) (a) Bischof, P. K.; Dewar, M. J. S. *J. Am. Chem. Soc.* **1975**, *97*, 2278–2280. (b) Hirao, K.; Yamabe, S. *Chem. Phys.* **1984**, *89*, 237–244.

(16) (a) Randon, L.; Poppinga, D.; Haddon, R. C. In *Carbonium Ions*; Olah, G. A.; Schleyer, P. v. R., Eds.; Wiley-Interscience: New York, 1976; Vol. 5, Chapter 38. (b) Hehre, W. J. In *Applications of Electronic Structure Theory*; Schaefer, H. F., III, Ed.; Plenum: New York, 1977; Chapter 7.

Table 1. Absolute Energies (–au) of C₂H₇⁺ Isomers and Other Species Discussed in This Work

| species | HF/6-31G*// | MP2(full)/6-31G*// | MP2(full)/6-31G**// | -/6-311G**//MP2(full)/6-31G** | | |
|------------------------------------------------|-------------|--------------------|---------------------|-------------------------------|-----------|-----------|
| | HF/6-31G* | MP2(full)/6-31G* | MP2(full)/6-31G** | MP2 | MP3 | MP4(sdtq) |
| 1 | 79.455 24 | 79.726 34 | 79.784 34 | 79.800 56 | 79.833 72 | 79.847 57 |
| 1a | 79.455 11 | 79.725 88 | 79.783 86 | 79.800 03 | 79.833 31 | 79.847 17 |
| 2 | 79.439 18 | 79.714 36 | 79.774 66 | 79.791 57 | 79.822 74 | 79.836 17 |
| 3 | 79.436 27 | 79.715 22 | 79.775 86 | 79.793 28 | 79.824 71 | 79.837 86 |
| 3a | | 79.715 22 | 79.775 86 | 79.793 26 | 79.824 67 | 79.837 82 |
| 4 | 79.427 22 | 79.712 18 | 79.773 98 | 79.791 31 | 79.822 01 | 79.835 16 |
| 5 | 79.432 37 | 79.711 99 | 79.772 65 | 79.789 92 | 79.821 29 | 79.834 40 |
| 6 | 79.428 38 | 79.712 83 | 79.772 87 | 79.789 94 | 79.820 37 | 79.834 02 |
| 7 | 79.452 87 | 79.717 11 | 79.774 39 | 79.789 44 | 79.824 20 | 79.838 92 |
| 16 | | | 79.752 55 | 79.769 64 | 79.821 29 | 79.818 09 |
| C ₂ H ₆ | 79.228 76 | 79.503 97 | 79.553 71 | 79.570 74 | 79.601 03 | 79.614 24 |
| C ₂ H ₅ ⁺ (8) | 78.309 94 | 78.561 45 | 78.601 18 | 78.613 27 | 78.640 27 | 78.653 21 |
| C ₂ H ₅ ⁺ (9) | 78.310 21 | 78.551 24 | 78.589 07 | 78.600 58 | 78.629 10 | 78.641 88 |
| CH ₅ ⁺ | 40.388 50 | 40.536 33 | 40.580 28 | 40.590 11 | 40.609 89 | 40.616 56 |
| CH ₄ | 40.195 17 | 40.337 04 | 40.369 86 | 40.379 14 | 40.398 18 | 40.404 84 |
| CH ₃ ⁺ | 39.230 64 | 39.329 44 | 39.351 20 | 39.356 10 | 39.374 80 | 39.379 56 |
| H ₂ | 1.126 83 | 1.144 14 | 1.157 66 | 1.160 26 | 1.166 21 | 1.168 10 |

Table 2. Relative Energies (kcal/mol) of C₂H₇⁺ Isomers

| species | HF/6-31G*// | MP2(full)/6-31G*// | MP2(full)/6-31G**// | -/6-311G**//MP2(full)/6-31G** | | | final ^a | exptl ^b |
|-------------------------------------------------------------|-------------|--------------------|---------------------|-------------------------------|--------|-----------|--------------------|--------------------|
| | HF/6-31G* | MP2(full)/6-31G* | MP2(full)/6-31G** | MP2 | MP3 | MP4(sdtq) | | |
| 1 | 0.00 | 0.00 | 0.00 | 0.00 | 0.00 | 0.00 | 0.33 | |
| 1a | 0.08 | 0.29 | 0.30 | 0.33 | 0.26 | 0.25 | 0.00 | 0.0 |
| 2 | 10.08 | 7.52 | 6.08 | 5.64 | 6.89 | 7.15 | 6.56 | |
| 3 | 11.91 | 6.98 | 5.32 | 4.57 | 5.65 | 6.09 | 4.43 | 7.8 |
| 3a | | 6.98 | 5.32 | 4.58 | 5.68 | 6.12 | 5.05 | |
| 4 | 17.59 | 8.89 | 6.50 | 5.81 | 7.35 | 7.79 | 5.77 | |
| 5 | 14.39 | 9.00 | 7.34 | 6.68 | 7.80 | 8.26 | 6.53 | |
| 6 | 16.86 | 8.48 | 7.20 | 6.67 | 8.38 | 8.50 | 7.16 | 13.0 |
| 7 | 1.49 | 5.79 | 6.24 | 6.98 | 5.97 | 5.43 | 3.15 | |
| 16 | | | 19.95 | 19.40 | 18.80 | 18.50 | 13.57 | |
| CH ₄ + CH ₃ ⁺ | 18.47 | 37.57 | 39.72 | 41.00 | 38.12 | 39.65 | 37.22 | 36 |
| H ₂ + C ₂ H ₅ ⁺ | 11.59 | 13.07 | 16.00 | 16.96 | 17.10 | 16.48 | 10.65 | 11.8 |
| C ₂ H ₆ + H ⁺ | 142.11 | 139.53 | 144.71 | 144.21 | 146.01 | 146.41 | 142.50 | 139.6 |

^a Final is MP4(sdtq)/6-311G**//MP2(full)/6-31G** corrected to 298 K including zero-point vibrational energy plus vibrational, rotational, translational, and expansion work (ΔpV) contributions to H_{298} . Scaled vibrational frequencies (by 0.93) were used, and RT/2 was assigned to each rotational and translational degree of freedom. ^b Values deduced or employed in ref 8.

than the C–H protonated form^{13a,15–18} but were inconclusive due to the technical limitations of the day. The theoretical levels employed for locating and characterizing the stationary points were inadequate, and some of the results are actually misleading. Hence, a systematic reexamination of this system is opportune. We employ *ab initio* molecular orbital theory at correlated levels to investigate geometries, energies, and vibrational frequencies of various C₂H₇⁺ structures as well as the possible mechanisms for H-scrambling and for decomposition into C₂H₅⁺ + H₂ and into CH₃⁺ + CH₄. We analyze the potential energy surface in greater detail than has been done previously and discuss the effects of basis sets and correlation on structure and relative energies. The computed vibrational frequencies are compared with Lee's experimental results.¹¹

Computational Methods

Optimizations and single-point calculations were carried out with the GAUSSIAN 90¹⁹ package of molecular orbital programs (and earlier versions) at Erlangen and at Calgary. Vibrational frequencies at MP2(full)/6-31G** were calculated with the CADPAC program.²⁰ Some geometries at HF/6-31G* and at MP2(full)/6-31G* already were available.^{21,22} All our additional structures were fully optimized at both these levels; the only constraints employed maintained the symmetries specified. Since the ions studied here have delocalized σ -electron systems involving hydrogens, the use of basis sets with polarization functions on

all atoms is desirable.²² Hence, all geometries were reoptimized at MP2(full)/6-31G**. The 6-31G** basis set also includes p-functions on all hydrogens; electron correlation effects are estimated at the full MP2 level. To refine the final relative energies, the MP2(full)/6-31G** geometries were further subjected to single-point MP4(SDTQ)/6-311G** calculations, i.e., with a triply split valence basis set and the Møller–Plesset (MP) perturbation treatment to complete (SDTQ) fourth order.²² These single-point calculations employed the frozen core approximation. The total and the relative energies are given in Tables 1 and 2, respectively.

The nature of each stationary point was characterized by vibrational analysis. The geometries of some structures changed significantly on going from the Hartree–Fock to the correlated optimization level. Hence, besides the HF/6-31G* vibrational analysis, we have computed the MP2(full)/6-31G** geometries as well. Zero-point energies, derived from the MP2(full)/6-31G** frequency calculations, are scaled (by 0.93)²³ and used to correct the relative energies. To assess enthalpy changes on going from 0 K to 298 K, $H - H_0$ was calculated at 298 K.²⁴ These values and zero-point energies are given in Table 3. Also given in Table 3 are the absolute entropies at 298 K. Our final relative energies are at MP4(SDTQ)/6-311G**//MP2(full)/6-31G** corrected to 298 K. Unless otherwise specified, these are the values discussed in the text. The structures we considered are shown in Figures 2 and 3.

(20) Amos, R. D.; Rice, J. E. *CADPAC: The Cambridge Analytic Derivatives Package*, Issue 4.0; Cambridge: U.K., 1987.

(21) *The Carnegie-Mellon Quantum Chemistry Archive*, 3rd ed.; Whiteside, R. A., Frisch, M. J., Pople, J. A., Eds.; Department of Chemistry, Carnegie-Mellon University, Pittsburgh, PA, 1983.

(22) For description of the basis set used in this work and Møller–Plesset perturbation theory, see: Hehre, W. J.; Radom, L.; Schleyer, P. v. R.; Pople, J. A. *Ab Initio Molecular Orbital Theory*; Wiley-Interscience: New York, 1986.

(23) Hout, R. F., Jr.; Levi, B. A.; Hehre, W. J. *J. Comput. Chem.* **1982**, *3*, 234–250.

(24) Enthalpy changes and absolute entropies were calculated with a program written by E. Kaufmann, based on the THERMO subroutine of MOPAC. We thank E. Kaufmann for furnishing us with the program.

(17) Köhler, H.-J.; Lischka, H. *Chem. Phys. Lett.* **1978**, *58*, 175–179.
 (18) Poirier, R. A.; Constantin, E.; Abbé, J. C.; Peterson, M. R.; Csizmadia, I. G. *J. Mol. Struct. (THEOCHEM)* **1982**, *88*, 343–355.
 (19) Frisch, M. J.; Head-Gordon, M.; Trucks, G. W.; Foresman, J. B.; Schlegel, H. B.; Raghavachari, K.; Robb, M. A.; Binkley, J. S.; Gonzales, C.; DeFrees, D. J.; Fox, D. J.; Whiteside, R. A.; Seeger, R.; Melius, C. F.; Baker, J.; Martin, R. L.; Kahn, L. R.; Stewart, J. J. P.; Topiol, S.; Pople, J. A. *Gaussian 90*; Gaussian Inc.: Pittsburgh, PA, 1990.

Table 3. Zero-Point Energies, Enthalpy Change, and Absolute Entropies of $C_2H_7^+$ Isomers^a

| species | ZPE (kcal/mol) | $H_{298} - H_0$ (kcal/mol) ^b | S (eu) ^b |
|----------------|------------------------|-----------------------------------------|-----------------------|
| 1 | 50.45 (0) ^c | 3.35 | 60.77 |
| 1a | 50.23 (1) | 2.99 | 60.03 |
| 2 | 49.64 (0) | 3.24 | 61.04 |
| 3 | 48.90 (1) | 2.91 | 59.19 |
| 3a | 48.98 (0) | 3.42 | 63.44 |
| 4 | 48.46 (1) | 2.99 | 59.61 |
| 5 | 48.77 (1) | 2.97 | 59.67 |
| 6 | 49.09 (1) | 3.04 | 59.99 |
| 7 | 48.09 (2) | 3.10 | 58.79 |
| 16 | 44.84 (1) | 3.70 | 64.51 |
| C_2H_6 | 45.28 (0) | 2.80 | 55.98 |
| $C_2H_5^+$ (8) | 36.87 (0) | 2.57 | 54.61 |
| CH_5^+ | 31.23 (0) | 2.73 | 52.08 |
| CH_4 | 27.20 (0) | 2.39 | 44.31 |
| CH_3^+ | 19.07 (0) | 2.38 | 44.51 |
| H_2 | 6.13 (0) | 2.07 | 31.32 |

^a All data were calculated using scaled (by 0.93) MP2(full)/6-31G** vibrational frequencies. ^b Includes vibrational, rotational, and translational contributions, where $RT/2$ was assigned to each rotational and translational degree of freedom. ^c In parentheses is given the number of imaginary frequencies.

Energies and Geometries

Previous theoretical investigations on the $C_2H_7^+$ cation concentrated on the C–C and C–H protonated structures 1 and 2 (Figure 2), presumed to be the two species observed experimentally. The high-level *ab initio* calculations of Raghavachari and co-workers gave a relative energy of 6.8 kcal/mol for the C–H (2) vs the C–C protonated species (1)^{13a} at MP4(SDTQ)/6-31G**//MP2(full)/6-31G*. The authors noted the dramatic differences between the structures optimized at the HF and the correlated level. Similar geometrical changes were reported earlier by Köhler and Lischka, who used the CEPA correlation method.¹⁷

The present work corroborates but also extends and modifies the previous results. We calculated both 1 (C_2) and 2 (C_2) to be minima. However, the C_s structure 1a, which is a transition state (at MP2(full)/6-31G**) for rotation of a CH_3 moiety, has essentially the same energy as 1. At our best level, 1a is more stable than 1 by 0.3 kcal/mol (Table 2). In the following discussion we will refer only to 1 (the minimum structure), but relative energies at 298 K are based on 1a. Optimization with polarization functions on hydrogens (MP2(full)/6-31G**) results only in small changes relative to the MP2(full)/6-31G* values (Table 4). At MP2(full)/6-31G**, the C–C distance in the C_2 structure 2 is 1.94 Å and the C–H–C angle is 105.3°. In the C_s structure 2, which is only a very loose complex at the HF/6-31G* level,^{13a} the distances between the hypercoordinated carbon and the three-center bonded hydrogen atoms are 1.215 and 1.193 Å at MP2(full)/6-31G** (Table 4). The relative energies also do not change much on optimization with the fully polarized basis set. At our highest level (Table 2), the C–C protonated structure (1) is more stable than the C–H protonated form (2) by 6.6 kcal/mol.

However, 2 is not the lowest C–H protonated minimum; the H_2 -rotated form 3 is more stable than 2. The C_s structure 3 is a minimum at HF/6-31G* but not at correlated levels, where the symmetry must be reduced to C_1 to eliminate the imaginary vibrational frequency. At MP2(full)/6-31G**, the C_s structure 3 is the transition state for the interconversion between the two degenerate C_1 forms (3a). Nevertheless, the C_s 3 and C_1 3a geometries differ very little and are almost indistinguishable energetically. The distances between the hypercoordinated carbon and the hydrogen atoms also involved in the three-center bonding are 1.206 Å in 3 and 3a. This value is very similar to the equivalent distances in 2. The differences between the optimized MP2(full)/6-31G** and HF/6-31G* structures in 3 are significant but not as large as those in 2 (Table 4).

The C_1 structure 3a was found to be more stable than the C_s 2 at all correlated levels. (Table 2 and Figure 4). This emphasizes the importance of including electron correlation in computational potential energy surface analysis. Poirier et al. found a structure similar to 3 to be a saddle point at 3-21G but commented that "this is probably an artifact of the basis set".¹⁸ Moreover, it was not possible to differentiate between 3 and 2. At our best level, 3 lies 4.4 kcal/mol above the global minimum 1 but is 2.1 kcal/mol more stable than 2. Hence, the second most stable form of protonated ethane is 3, with the H_2 attached perpendicular to the C–C bond rather than eclipsed (as in 2).

Although the point is a minor one, we searched extensively for the transition state between structures 2 and 3, both of which are minima. Since all the transition-state optimizations either converged to unrelated geometries or did not converge at all, we carried out a series of restrained geometry optimizations with fixed C–C–H_a–H_b dihedral angle (see structures in Table 4). The H–H moiety was rotated step by step from 180° (2) to 90° (3), and each geometry was optimized at the correlated MP2(full)/6-31G* level. We found a geometry with a dihedral angle of 153° to be the highest in energy, but only 0.14 kcal/mol above 2. The small energy difference between this geometry and 2 suggests that the transition state interconnecting 2 and 3 must be closely related, structurally and energetically, to both these minima. The energy surface around these stationary points is very flat. All our evidence indicates that the barrier leading from 2 to 3 should be very low. Hence, only the more stable structure 3 should be experimentally accessible.

How easily do the hydrogen atoms exchange? This question is central to the interpretation of the results of Saunders, Cross, et al.¹⁰ Several processes are involved. First, the four nonequivalent hydrogen atoms on the hypercoordinated carbon in 3 exchange by rotation of the CH_4 group around the C–C bond: transition structures 4 and 5 have C_s symmetry and a single negative eigenvalue in the force constant matrix. Their relative energies lie respectively 1.3 and 2.1 kcal/mol above 3 and 5.8 and 6.5 kcal/mol above the global minimum 1. Second, the C_s structure 6 is the transition state for interconversion of the two minima, 1 and 2. The geometry of 6 is rather similar to that of 2. Our best result indicates that the energy of 6 is 7.2 kcal/mol higher than that of 1 and 2.7 kcal/mol above 3. Third, the rotation of the methyl groups in 1, via the C_s structure 1a as transition state, occurs with a barrier of only 0.3 kcal/mol (Table 2). Hence, the energies of all transition states, those interconnecting the minima as well as those for hydrogen exchange, lie lower than the dissociation energy into $C_2H_5^+$ and H_2 . We calculate the latter to be 10.7 kcal/mol relative to the global minimum 1. These results agree with Kebarle's experimental dissociation energies of 10.5 ± 27^c and 13 kcal/mol⁸ and also are consistent with the qualitative observations of Saunders et al.¹⁰

The D_{3d} structure 7, with a linear C–H–C bond, is a minimum at HF/6-31G* but not at correlated levels. Its relative energy is 3.2 kcal/mol above 1. Since the H-bridged (C_{2v} , 8) ethyl cation is the only $C_2H_5^+$ minimum at correlated levels (the classical form 9 is a minimum at, e.g., HF/6-31G* but not at MP2/6-31G*),^{13a} we also tried a set of $C_2H_5^+ \cdot H_2$ complexes in C_{2v} symmetry (Figure 3). Structures 10 and 11 (which have exactly the same energy) are both minima at MP2(full)/6-31G**, but they are very loose complexes (Table 5). At that level, the dissociation energies of 10 and 11 into $C_2H_5^+$ (8) + H_2 at 0 K are very small (<0.1 kcal/mol). 12 is a transition state for motion of the H_2 moiety parallel to the C–C bond, whereas 13 is a higher order stationary point. Their energies are also given in Table 5. Another possibility for complexation of H_2 to $C_2H_5^+$ is in a less symmetrical C_s form. Structures 14 and 15 (Figure 3) were located as stationary points; however, only 14 is a minimum. 15 is the transition structure for rotation of the H_2 moiety. Starting from the C_s structures 14 and 15, we tried to find transition states for the addition of H_2 to the ethyl cation. Optimizations in C_s symmetry led to structures 16 and 17 (Figure 3). However, only

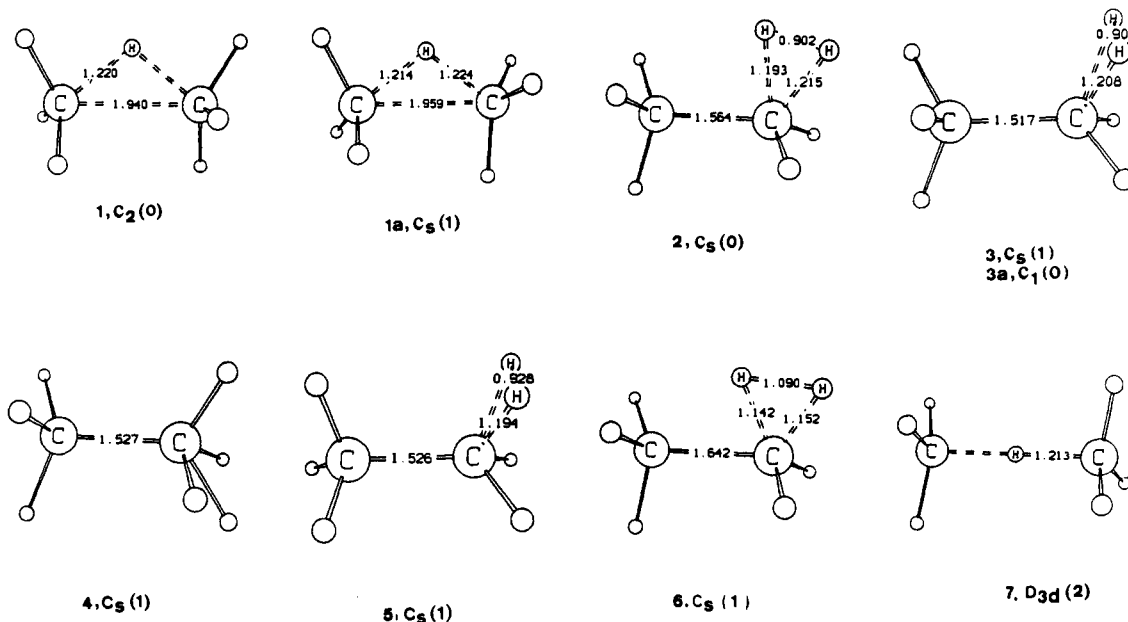


Figure 2. MP2(full)/6-31G** geometries of $C_2H_7^+$ isomers. The number of imaginary frequencies is given in parentheses.

16 is a true transition state; 17 has two negative values in the force constant matrix. At our highest level, 16 lies 2.9 kcal/mol above the ethyl cation 8 and H_2 (Table 5). 17 has essentially the same energy as 16. We also tried structures where the H_2 approaches the ethyl cation from above. Nevertheless, no minimum or transition state was found. All optimizations in C_s symmetry converged to structures which have two or more imaginary frequencies. The low dissociation energies of the complex-like minima 10, 11, and 14 indicate that the H_2 acts as a solvation species around the ethyl cation. These complexes are not expected to be observed experimentally, since the entropic contribution to the energy at any measurable temperature should exceed the small binding energy.

Figure 4 shows the dependence of the relative energies of the bonded species vs theoretical level, with the H-bridged structure 1 taken as the reference. Also included in Figure 4 are values for $CH_4 + CH_3^+$ and $H_2 + C_2H_5^+$. While the relative energies of $CH_4 + CH_3^+$ and of $C_2H_5^+ + H_2$ vary widely, those of the five structures 2–6 remain clustered together. Inclusion of electron correlation at, e.g., MP2(full)/6-31G*, has the largest effect, which is drastic on the relative energy of CH_3^+ and CH_4 .

Vibrational Frequencies

Recently, we compared experimental and theoretical vibrational spectra to establish the H-bridged structures of the *sec*-butyl²⁵ and cyclooctyl cations.²⁶ The experimental vibrational spectra of $C_2H_7^+$ ions, reported by Lee et al.,¹¹ invite comparisons with our computed data. Table 6 gives the calculated vibrational frequencies for the three minima 1, 2, and 3a as well as for the methonium cation CH_5^+ in the equilibrium C_s geometry. The experimental data of Lee et al.¹¹ also are given in this table.

As shown in Table 6a, the three vibrational frequencies assigned by Lee et al. to the C–C protonated species 1 are reproduced nicely by our calculations. The differences between the experimental and the scaled theoretical frequencies are only about 10 cm^{-1} for the three peaks. Of great interest are the vibrations computed at 2042 and 1976 cm^{-1} . As has been shown earlier, IR peaks in this region of the spectrum are characteristic of C–H vibrations in symmetrically 1,2-H-bridged²⁵ and in transannularly

bridged²⁶ structures. In the present case, the frequency at 2042 cm^{-1} is assigned to the motion of the bridging H parallel to the C–C axis and that at 1976 cm^{-1} to the bridging H moving away from the C–C axis. The large calculated intensities indicate that these vibrations should be prominent in the IR spectrum of the $C_2H_7^+$ ion. Unfortunately, the laser employed by Lee et al. did not permit study below 2400 cm^{-1} .

While the calculated and experimental spectra agree very well for the bridged structure 1, the same is *not* true for the C–H protonated cation (either 2 or 3). First, we did not compute any vibration above 3100 cm^{-1} for either 2 or 3, whereas Lee et al. observed a peak at 3964 cm^{-1} and assigned it to the H–H stretching in a loose $C_2H_5^+ \cdot H_2$ complex.¹¹ Second, also in contrast to the results of Lee et al., our highest frequencies in 2 and 3 (see Table 6b and c) are not due to H–H stretching but are due to an asymmetric C–H stretch in the CH_3 moiety. The characteristic frequencies associated with the hydrogens in the three-center bond appear more than 1000 cm^{-1} below that claimed by Lee et al. The vibrational frequencies at 2770 cm^{-1} for 2 and 2716 cm^{-1} for 3 are due mainly to H–H stretching. The asymmetrical C–H stretching motions in these three-center bonds give rise to the frequencies at 2229 cm^{-1} for 2 and at 2217 cm^{-1} for 3 (Tables 6b and c).

To check these results at different theoretical levels, we also calculated the vibrational frequencies for 1 and 3 with a double- ζ plus polarization basis set and the CISD electron correlation method (Table 6a and c). The results strongly support our conclusions and also the unpublished frequency calculations of Dupuis, mentioned by Lee et al.¹¹ While disagreeing with the experimental assignment, our results appear to be much more plausible when they are compared with those of other H_2 complexes, e.g., the computed spectra of the CH_5^+ ion. As shown in Table 6d, the vibrational spectrum of CH_5^+ correlates well with those of 2 and 3. In the C_s form of the CH_5^+ ion, the H–H stretching vibration is found at 2619 cm^{-1} , while a C–H stretching mode appears at 2382 cm^{-1} . Schreiner et al. have analyzed the vibrational spectrum of the CH_5^+ cation recently.^{13c,27} They also conclude that the H–H stretching vibration in the three-center bonds lies below 3000 cm^{-1} (the scaled frequencies are 2633 cm^{-1} for the C_s (1) species).

The geometrical parameters given in Table 4 (as well as the energy data) indicate that in 2 and 3 the H_2 moiety is rather tightly bound to the $C_2H_5^+$ cation, that is, a true $C_2H_7^+$ species

(25) Buzek, P.; Schleyer, P. v. R.; Sieber, S.; Koch, W.; Carneiro, J. W. de M.; Vancik, H.; Sunko, D. E. *J. Chem. Soc., Chem. Commun.* **1991**, 671–674.

(26) Buzek, P.; Schleyer, P. v. R.; Vancik, H.; Sunko, D. E. *J. Chem. Soc., Chem. Commun.* **1991**, 1538–1540.

(27) Also see: Komornicki, A.; Dixon, D. A. *J. Chem. Phys.* **1987**, *103*, 5625–5634.

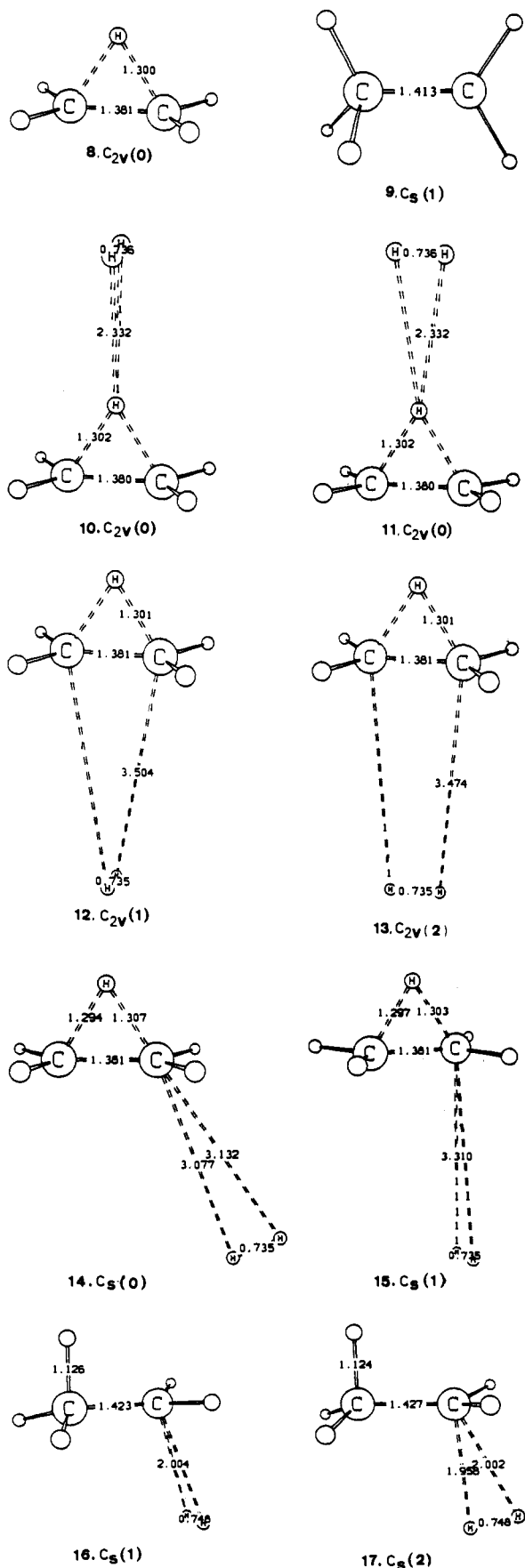


Figure 3. MP2(full)/6-31G** geometries of ethyl cation isomers and $C_2H_5^+ \cdot H_2$ complex-like structures. The number of imaginary frequencies is given in parentheses.

is involved and not just a loose $C_2H_5^+ \cdot H_2$ complex. At all correlated levels, the C-H bond lengths in the three-center bonds are about 1.2 Å, whereas the H-H distances are about 0.9 Å.

Table 4. Selected Geometrical Parameters for $C_2H_7^+$ and CH_5^+ ^a

| | HF/ 6-31G* | MP2 (full)/ 6-31G* | MP2 (full)/ 6-31G** |
|--|---------------|--------------------------|---------------------------|
| | 2.163 | 1.953 | 1.940 |
| | 1.239 | 1.225 | 1.220 |
| | 121.56 | 105.67 | 105.29 |
| | 1.519 | 1.518 | 1.517 |
| | 1.289 | 1.216 | 1.205 |
| | 1.289 | 1.217 | 1.206 |
| | 0.814 | 0.896 | 0.906 |
| | 1.434 | 1.565 | 1.564 |
| | 2.676 | 1.199 | 1.193 |
| | 2.734 | 1.222 | 1.215 |
| | 0.733 | 0.901 | 0.902 |
| | 1.230 | 1.185 | 1.177 |
| | 1.229 | 1.182 | 1.177 |
| | 0.853 | 0.950 | 0.957 |

^a Distances in angstroms; angles in degrees.

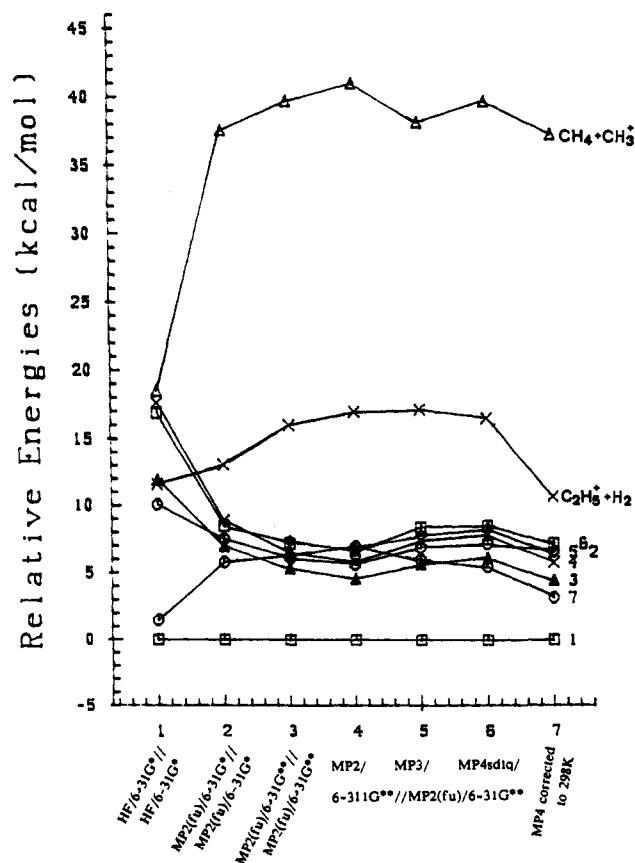


Figure 4. Relative energies of $C_2H_7^+$ isomers as a function of the theoretical level.

Consistent with the shift of the H-H stretching vibration to lower frequencies, the three-center C-H distances in the CH_5^+ ion are smaller and the H-H distance is greater than those in $C_2H_7^+$.

Table 5. Energies of the Complex-like Structures 10–17 Relative to $C_2H_5^+ + H_2^a$

| species | MP2(full)/6-31G**// MP2(full)/6-31G** | MP2(full)/6-31G**// MP2(full)/6-31G** + ZPE |
|--------------|------------------------------------------|------------------------------------------------|
| 10, C_{2v} | -0.94 (0) | -0.05 |
| 11, C_{2v} | -0.95 (0) | -0.08 |
| 12, C_{2v} | -0.39 (1) | -0.04 |
| 13, C_{2v} | -0.35 (2) | -0.09 |
| 14, C_s | -0.51 (0) | 0.07 |
| 15, C_s | -0.42 (1) | -0.02 |
| 16, C_s | 3.95 (1) | 2.92 ^b |
| 17, C_s | 4.09 (2) | 5.90 |

^a Energies are in kcal/mol. In parentheses is given the number of imaginary frequencies at MP2(full)/6-31G**. ^b MP4sdq/6-311G**/MP2(full)/6-31G** corrected to 298 K.

Our results on CH_5^+ agree with the earlier findings.^{13c,27} Based on the experimental bonding energy of $C_2H_7^+$ (4 kcal/mol relative to $C_2H_5^+ + H_2$),⁸ Lee et al. claimed that their 3964-cm⁻¹ frequency agrees with observations for other AH_2 complexes (e.g., H_5^+ and H_7^+).¹¹ We calculate an energy of 6.2 kcal/mol (at 298 K) for the decomposition of $C_2H_7^+$ (3) into $C_2H_5^+$ (8) and H_2 (see Table 7 and Discussion below). However, since 2 and 3 are best considered as H_2 complexes of a classical ethyl cation (9), comparisons of bonding energy should be made on this basis. A "classical" $CH_3CH_2^+$ rotation transition structure can be computed if C_s symmetry and a 0° H-C-C-H dihedral angle are imposed. At MP2(full)/6-31G**, the bridged structure 8 is more stable than the classical 9 by 6.7 kcal/mol (at 0 K). Thus, the actual bonding energy of $C_2H_7^+$ (3) should be about 13 kcal/mol. As a consequence, the H-H stretching vibration occurs at much lower frequency than in free H_2 . We conclude that the experimental vibrational spectrum¹¹ of the second $C_2H_7^+$ species does not correspond to that of 3 (or 2). In addition, the complex-like structures 10, 11, and 14 (Figure 3) are too weakly bonded to be responsible for the second $C_2H_7^+$ species detected experimentally.

Discussion

Hiraoka and Kebarle⁸ and Poirier et al.¹⁸ summarized their $C_2H_7^+$ results in an energy diagram. Our revised version (Figure 1) contains the same information but is based on newer literature energies for reference compounds (Table 8). Some discrepancies between our theoretical results and those derived from the high-pressure mass spectrometry experiments⁸ are evident. Our 4.4 kcal/mol (corrected to 298 K) energy difference between the two stable minima is less than the 7.8 kcal/mol deduced from experiment.⁸ Likewise, the calculated 2.7 kcal/mol barrier for rearrangement from 3 to 1, assumed to proceed via structure 6, is lower than the experimental value of 5.2 kcal/mol.⁸ Also contrary to Kebarle, we computed a barrier of 2.9 kcal/mol (Table 5) for the addition of H_2 to the ethyl cation leading to 3 (see below).

Table 7 summarizes the thermochemical data for eq 3. Our energy for this process diverges by about 2.4 kcal/mol from the value Kebarle reported but is in excellent agreement with more recent data.^{28,29} The value of 219 kcal/mol assumed by Kebarle for the heat of formation of the ethyl cation has been revised more recently to 216 kcal/mol.^{28–32} (see Table 8). Also given in Table 7 are thermochemical data for the dissociations of $C_2H_7^+$ and CH_5^+ into $C_2H_5^+ + H_2$ and $CH_3^+ + H_2$, respectively (eqs 4 and 5).

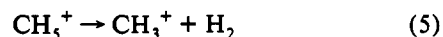
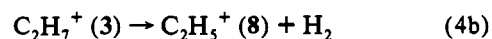
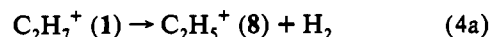
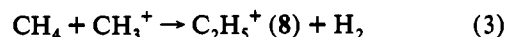
(28) Lias, S. G.; Liebman, J. F.; Levin, R. D. *J. Phys. Chem. Ref. Data* 1984, 13, 695–808.

(29) Traeger, J. C.; McLoughlin, R. G. *J. Am. Chem. Soc.* 1981, 103, 3647–3652.

(30) Baer, T. *J. Am. Chem. Soc.* 1980, 102, 2482–2483.

(31) Bohme, D. K.; Mackay, G. I. *J. Am. Chem. Soc.* 1981, 103, 2173–2175.

(32) Rosenstock, H. M.; Buff, R.; Ferreira, M. A. A.; Lias, S. G.; Parr, A. C.; Stockbauer, R. L. *J. Am. Chem. Soc.* 1982, 104, 2337–2345.



For the dissociation of $C_2H_7^+$ (1) into $C_2H_5^+$ (8) + H_2 (eq 4a), our theoretical enthalpy and Kebarle's directly measured experimental value differ hardly at all (about 1.0 kcal/mol). However, for reaction 4b, the theoretical enthalpy is 2.2 kcal/mol greater than the experimental value (Table 7). The experimental reactions enthalpies and entropies were derived from van't Hoff plots of the measured equilibria. We have not found any consistent difference between experiment and our theoretical results. Note that, for reaction 4b, whereas ΔH and ΔS do not agree at all, the experimental (-1.8 kcal/mol) and the theoretical (-1.2 kcal/mol) free energies (at 298 K) are in reasonable agreement. The dissociation of CH_5^+ is calculated to involve an enthalpy change of 38.9 kcal/mol at 298 K. Nevertheless, in recent high-level calculations on CH_5^+ , Schleyer and Carneiro^{13b} found the dissociation energy of CH_5^+ to be 42.0 kcal/mol. Kebarle reports a value of 40 kcal/mol for this process; however, more recent experimental data^{29,33} lead to an upward revision to 42.5 kcal/mol at 298 K (Table 7). Pople and Curtiss's theoretical heats of formation of small cations agree on average within 2 kcal/mol of the experimental values,³⁴ but for CH_5^+ the authors calculated a heat of formation (at 298 K) 5.5 kcal/mol greater than the experimental value. Pople's data yield a value of 38.6 kcal/mol (at 298 K) for the dissociation energy of CH_5^+ . Our result is closer to that deduced from the more recent experimental determinations.

We have also searched for the elimination pathways of H_2 and CH_3^+ from $C_2H_7^+$ (as well as the pathways for the corresponding reverse reactions for addition). Together with the isomerizations of the $C_2H_7^+$ system discussed above, these processes characterize reaction 1 mechanistically.

We have not carried out dynamics calculations but have explored two possible pathways for the CH_3^+ addition to CH_4 (Figure 5). The first one involves a C_{3v} symmetric approach, in which a hydrogen atom of the CH_4 interacts as donor with the vacant p-orbital of the CH_3^+ cation (Figure 5a). However, no local minimum in C_{3v} was found and, as described below, distortion from C-H-C linearity leads to the C_2 symmetry structure 1. The second pathway in C_s symmetry involves a side-on interaction of the methyl cation p-orbital with a C-H bond of methane (Figure 5b). When this approach was tested computationally, also by starting the optimization with a reasonably large separation, only structure 1 resulted. At large and fixed C-C distances (>2.43 Å), the most stable $C_2H_7^+$ form is one with a linear C-H-C geometry (cf. Figure 5a). When the carbon atoms are allowed to approach each other, this structure begins to distort and the optimization converges to structure 1 with the central hydrogen atom placed symmetrically between both carbons. These results indicate that the addition of CH_4 to CH_3^+ leads directly to the more stable C_2 structure 1.

In their cross-beam electron accelerator experiments, Saunders et al.¹⁰ started with deuterium-labeled methane or methyl cation (reactions 6a and 6b). The distribution of isotopically labeled product ions was investigated as a function of collision energy. Extensive hydrogen-deuterium scrambling occurred at low collision energies. However, as the collision energy increased, the deuterium distribution (see eqs 6a and 6b) became nonrandom. $C_2H_2D_3^+$ predominated in eq 6a and $C_2H_3D_2^+$ in eq 6b.

(33) Bohme, D. K.; Mackay, G. I.; Schiff, H. I. *J. Chem. Phys.* 1980, 73, 4976–4986.

(34) Pople, J. A.; Curtiss, L. A. *J. Phys. Chem.* 1987, 91, 155–162.

Table 6. Theoretical Vibrational Frequencies for 1, 2, 3, and the CH₅⁺ Ion^a

| (a) Compound 1 | | | | | |
|-------------------------------|-----------|-------------------------------|-----------|---------------------|-------------------------------------------------------------------------|
| scaled frequency ^b | intensity | scaled frequency ^c | intensity | exptl ¹¹ | approximate normal mode description |
| 3139 | 45.83 | 3125 | 19.37 | | asym CH stretch of CH ₃ , asym CH ₃ s |
| 3136 | 12.55 | 3127 | 7.73 | 3128 | asym CH stretch of CH ₃ , sym CH ₃ s |
| 3078 | 44.47 | 3083 | 23.23 | | asym CH stretch of CH ₃ , sym CH ₃ s |
| 3075 | 12.50 | 3074 | 16.09 | 3082 | asym CH stretch of CH ₃ , asym CH ₃ s |
| 2936 | 30.77 | 2939 | 15.85 | 2945 | sym CH stretch of CH ₃ , asym CH ₃ s |
| 2935 | 1.77 | 2990 | 0.39 | | sym CH stretch of CH ₃ , sym CH ₃ s |
| 2042 | 49.88 | 2117 | 251.35 | | asym CH stretch of bridging proton |
| 1976 | 43.68 | 1933 | 18.71 | | sym CH stretch of bridging proton |
| 1410 | 2.55 | 1424 | 0.66 | | asym ∠HCH bend of CH ₃ , asym CH ₃ s |
| 1408 | 3.09 | 1425 | 1.05 | | asym ∠HCH bend of CH ₃ , sym CH ₃ s |
| 1393 | 30.32 | 1412 | 26.08 | | asym ∠HCH bend of CH ₃ , sym CH ₃ s |
| 1387 | 40.18 | 1407 | 31.77 | | asym ∠HCH bend of CH ₃ , asym CH ₃ s |
| 1316 | 0.27 | 1313 | 0.43 | | sym ∠HCH bend of CH ₃ (umbrella mode), sym CH ₃ |
| 1246 | 5.40 | 1248 | 31.57 | | sym ∠HCH bend of CH ₃ (umbrella mode), asym CH ₃ |
| 1097 | 14.79 | 1109 | 10.23 | | asym CH ₃ out-of-plane rock - proton out-of-plane distortion |
| 1071 | 0.24 | 1086 | 0.06 | | CH ₃ out-of-plane rock, sym CH ₃ s |
| 991 | 62.36 | 998 | 131.25 | | CH ₃ in-plane rock, asym CH ₃ s |
| 815 | 3.32 | 817 | 2.14 | | CH ₃ in-plane rock, sym CH ₃ s |
| 343 | 4.78 | 331 | 4.02 | | CC stretch (- sym CH stretch of bridging H) |
| 263 | 6.37 | 190 | 3.95 | | asym CH ₃ out-of-plane rock + proton out-of-plane distortion |
| 236 | 2.01 | 213 | 0.85 | | CC bond twist |

| (b) Compound 2 | | |
|-------------------------------|-----------|--------------------------------------------------------------------------------------------|
| scaled frequency ^b | intensity | approximate normal mode description |
| 3085 | 39.29 | asym CH stretch of CH ₂ + asym CH stretch of CH ₃ |
| 3067 | 0.02 | asym CH stretch of CH ₃ |
| 3059 | 10.61 | asym CH stretch of CH ₃ |
| 2991 | 30.63 | sym CH stretch of CH ₂ |
| 2951 | 1.56 | sym CH stretch of CH ₃ (breathing mode) |
| 2770 | 17.49 | HH stretch of H ₂ in the three-center bond |
| 2229 | 34.72 | asym CH stretch of CH in the three-center bond |
| 1536 | 10.67 | bend of CH ₂ - ∠HCH bend in the three-center bond (umbrella) |
| 1443 | 13.47 | sym ∠HCH bend of CH ₃ |
| 1442 | 9.53 | asym ∠HCH bend of CH ₃ + asym ∠HCH bend of CH ₂ |
| 1417 | 3.79 | sym ∠HCH bend of CH ₂ |
| 1371 | 29.35 | asym ∠HCH bend in CH ₂ - asym ∠HCH bend of CH ₃ |
| 1369 | 1.26 | sym ∠HCH bend of CH ₃ (umbrella mode) |
| 1165 | 0.69 | asym ∠HCH bend in CH ₃ - asym ∠HCH bend in CH ₂ |
| 1119 | 11.04 | CH ₃ in-plane rock + CH ₂ -H ₂ in-plane rock |
| 935 | 71.23 | CH ₃ in-plane rock - CH ₂ -H ₂ in-plane rock + CC stretch |
| 869 | 5.29 | CH ₃ out-of-plane rock + CH ₂ -H ₂ out-of-plane rock |
| 780 | 33.23 | CC stretch + CH ₂ -H ₂ in-plane rock |
| 625 | 126.37 | CH ₃ in-plane rock - H ₂ in-plane rock |
| 289 | 12.90 | CC bond twist + CH ₂ twist + H ₂ C twist |
| 221 | 23.52 | H ₂ twist |

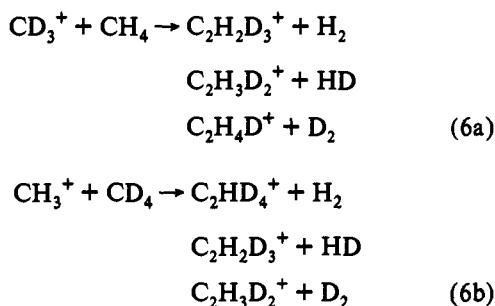
| (c) Compound 3 | | | | | |
|-------------------------------|-----------|-------------------------------|-----------|-------|---------------------------------------------------------------------------------------|
| scaled frequency ^b | intensity | scaled frequency ^c | intensity | exptl | approximate normal mode description |
| 3061 | 1.73 | 3041 | 0.00 | 2762 | asym CH stretch in CH ₃ |
| 3051 | 4.88 | 3030 | 1.03 | 2683 | asym CH stretch in CH ₃ |
| 2967 | 55.89 | 2975 | 41.61 | 2825 | asym CH stretch in CH ₂ |
| 2952 | 0.76 | 2961 | 0.60 | 2521 | sym CH stretch of CH ₃ (CH ₃ breathing mode) |
| 2929 | 46.18 | 2981 | 31.24 | 2601 | sym CH stretch of CH ₂ - HH stretch of H ₂ -CH ₂ |
| 2716 | 28.42 | 2832 | 16.89 | 3964 | HH stretch of H ₂ -CH ₂ + sym CH stretch of CH ₂ |
| 2217 | 54.68 | 2094 | 60.74 | | asym CH stretch of H ₂ -C in three-center bond |
| 1520 | 0.88 | 1514 | 0.55 | | ∠HCH bend of CH ₂ - sym CH stretch of H ₂ -C |
| 1444 | 13.81 | 1461 | 7.42 | | asym ∠HCH bend of CH ₃ |
| 1441 | 16.24 | 1458 | 12.96 | | asym ∠HCH bend of CH ₃ |
| 1391 | 3.92 | 1408 | 4.44 | | sym ∠HCH bend of CH ₃ (umbrella) + sym ∠H-C-H ₂ bend (umbrella) |
| 1328 | 5.03 | 1340 | 6.25 | | sym ∠HCH bend of CH ₃ (umbrella) - sym ∠H-C-H ₂ bend (umbrella) |
| 1282 | 18.46 | 1210 | 18.14 | | asym ∠HCH bend in CH ₃ + asym ∠HCH bend in CH ₂ |
| 1198 | 32.38 | 1318 | 18.41 | | CH ₂ twist - H ₂ -C rock in H ₂ -CH ₂ |
| 1105 | 5.86 | 1133 | 3.87 | | CH ₃ out-of-plane rock + CH ₂ -H ₂ out-of-plane rock |
| 1013 | 23.11 | 1047 | 18.31 | | CH ₃ in-plane rock + CC stretch |
| 908 | 21.45 | 927 | 17.25 | | CC stretch - CH ₃ in-plane rock |
| 740 | 22.01 | 760 | 16.77 | | CH ₃ out-of-plane rock - CH ₂ -H ₂ out-of-plane rock |
| 677 | 72.15 | 686 | 48.44 | | CH ₃ in-plane rock - CH ₂ -H ₂ in-plane rock |
| 259 | 0.41 | 282 | 0.95 | | CC bond twist + CH ₂ twist + H ₂ -C twist |
| 66 | 70.14 | 172 | 44.47 | | CC bond twist - H ₂ -C twist + CH ₂ rock |

| (d) CH ₅ ⁺ Ion | | |
|--------------------------------------|-----------|------------------------------------------------------------------------------------|
| scaled frequency ^b | intensity | approximate normal mode description |
| 3107 | 85.60 | asym CH stretch of CH ₃ |
| 3015 | 79.77 | asym CH stretch of CH ₃ |
| 2892 | 101.97 | sym CH stretch of CH ₃ (breathing mode) + CH stretch of CH ₂ |

Table 6 (Continued)

| (d) CH ₅ ⁺ Ion | | |
|--------------------------------------|-----------|-------------------------------------------------------------------------------------------------------------|
| scaled frequency ^b | intensity | approximate normal mode description |
| 2619 | 36.44 | sym CH stretch of CH ₂ + H ₂ stretch + CH stretch of CH ₃ (breathing mode) |
| 2382 | 64.14 | asym CH stretch of CH ₂ |
| 1507 | 6.35 | ∠HCH bend of CH ₂ - sym ∠HCH bend of CH ₃ (umbrella) |
| 1422 | 0.03 | asym ∠HCH bend of CH ₃ |
| 1403 | 0.92 | sym ∠HCH bend of CH ₃ |
| 1258 | 58.15 | CH ₃ out-of-plane rock + H ₂ out-of-plane rock |
| 1228 | 34.24 | sym ∠HCH bend of CH ₃ (umbrella) |
| 710 | 243.52 | CH ₃ in-plane rock - H ₂ stretch |
| 305 | 49.14 | H ₂ twist |

^a Vibrational frequencies are in cm⁻¹; intensities are in km/mol. ^b Frequencies calculated at the MP2(full)/6-31G** level, scaled by 0.93. ^c Frequencies calculated at the DZ+P/CISD level, scaled using out-of-plane and bending mode internal coordinate scaling factors.



These results were interpreted in terms of C₂H_nD_{7-n}⁺ (n = 2, 3, 4) intermediates. At low collision energies, the rate of hydrogen-deuterium scrambling is fast relative to the rate of decomposition. As a consequence, a statistical distribution of isotopically labeled products results. As the relative collision energy increases, however, there is less time for total scrambling. This leads to a nonrandom isotopic distribution in the final products. This nonrandom product distribution found at higher energy led Saunders et al. to assume that the intermediate species has a structure like **3** (or **2**), with the extra proton associated with only a single carbon atom. They argued that the symmetrical structure **1** would lead (via reaction 6a) to equimolar formation of C₂H₃D₂⁺ and C₂H₂D₃⁺ (if bridging hydrogen participates in the dissociation) or to C₂H₄D⁺ and C₂H₂D₃⁺ (if bridging hydrogen did not participate in the dissociation). Similar behavior should be expected for reaction 6b (in which the Hs and Ds in the initial reactants are interchanged).¹⁰

Our calculational results indicate that **1** (rather than **2** or **3**) is the first species formed from the methyl cation and methane. The rearrangement from **1** into **3** involves transition state **6** (7.2 kcal/mol above **1**), leading, via **2** (6.6 kcal/mol above **1**), to **3**. The rotation of the CH₄ group around the C-C bond in **3** renders all the hydrogens bonded to the hypervalent carbon equivalent. The barrier is 1.3 kcal/mol (transition structure **4**). Although **2**, as well as **3**, already has partial H-H bonding (one of the Hs comes from the bridging position, see structure **6**), the interchange between the hydrogens in the hypervalent carbon involves a lower barrier (1.3 kcal/mol) than the return to **1** (2.7 kcal/mol). The low vibrational frequency calculated for the H-H stretching in the three-center bonds also indicates the H-H bonding to be only partial. If the hydrogens bonded to the hypervalent carbon interchange, any pair of them can be lost to form the C₂H₅⁺ ion.

If, as the calculations indicate, partial scrambling in the CH₄ moiety is easier than the total scrambling, it is possible to reconcile Saunders's experimental results with the initial formation of **1**. Consider the isotopic labeled reactions 6a and 6b. For reaction 6a, after rearrangement of **1** into **3**, we will have an equal amount of CD₃-CH₄⁺ and of CH₃-CHD₃⁺. Assuming all the Hs in CD₃-CH₄⁺ to be equivalent, decomposition into ethyl cation and H₂ would give C₂H₂D₃⁺ as the only product. On the other side, decomposition of CH₃-CHD₃⁺ leads to both C₂H₃D₂⁺ and C₂H₄D⁺. This means that statistically we will observe a predominance of C₂H₂D₃⁺ over C₂H₃D₂⁺ (as well as over C₂H₄D⁺)

Table 7. Thermochemical Data for Reactions 3-5^a

| reaction | theor ^b | | exptl ^c | |
|------------------------------------------------------------------------------|--------------------|------|--------------------|------------|
| | ΔH | ΔS | ΔH | ΔS |
| CH ₄ + CH ₅ ⁺ = | -26.6 | -2.9 | -24.2 | |
| C ₂ H ₅ ⁺ (8) + H ₂ | | | -27.3 ^d | |
| C ₂ H ₇ ⁺ (1) = | 10.7 | 25.2 | 11.8 ± 0.4 | 25 ± 1 |
| C ₂ H ₅ ⁺ (8) + H ₂ | 11.4 ^e | | | |
| C ₂ H ₇ ⁺ (3) = | 6.2 | 26.7 | 4.0 ± 0.5 | 19.6 ± 1.5 |
| C ₂ H ₅ ⁺ (8) + H ₂ | 7.3 ^e | | | |
| CH ₅ ⁺ = CH ₃ ⁺ + H ₂ | 38.9 | 23.8 | 40.0 | |
| | 42.0 ^e | | 42.5 ^f | |
| | 38.6 ^g | | | |

^a All data are at 298 K; ΔH in kcal/mol; ΔS in eu. ^b This work. MP4(sdtq)/6-311G**//MP2(full)/6-31G** corrected to 298 K. ^c Reference 8. ^d ΔH_f of C₂H₅⁺ = 216 kcal/mol; ΔH_f of CH₃⁺ = 261.3 kcal/mol (ref 29); ΔH_f of CH₄ = -18 kcal/mol (ref 28). ^e At 0 K, ref 15b. ^f ΔH_f of CH₅⁺ = 218.8 kcal/mol (ref 33); ΔH_f of CH₃⁺ = 261.3 kcal/mol (ref 29). ^g Reference 34.

by a factor of 2 (assuming no isotope effect). This agrees with the experiment of Saunders et al.¹⁰ The same interpretation can be applied to reaction 6b if the Hs and Ds are interchanged. In this case the main product is C₂H₃D₂⁺.

We also investigated possible pathways for H₂ elimination from C₂H₇⁺. It is inherently likely that C₂H₇⁺ loses H₂ by 1,1-elimination, since **3** has the form of a C₂H₅⁺-H₂ complex. Reasoning from the other direction, H₂ would have to attack the bridged form of the C₂H₅⁺ cation, which is the only minimum at correlated levels.^{13a} Since 1,2-H₂ attack in C_{2v} symmetry (via structures **10**-**13**) is forbidden, the most probable pathway would be a less symmetrical attack concerted with movement of the bridging H in C₂H₅⁺ (**8**). Here we investigate two pathways (Figure 6). In the first, the H₂ approaches the ethyl cation from the backside in C_s symmetry (pathway A in Figure 6). Starting from **15** we could locate the transition state **16**, 2.9 kcal/mol above the bridged ethyl cation **8** and H₂. Starting from the H₂ rotated structure **14**, **17** is found, but it has two negative eigenvalues in the force constant matrix. The energy of **17** is very similar to that of **16** (Table 5). In the second pathway, the H₂ molecule approaches the ethyl cation from above (pathway B in Figure 6). We could locate two stationary points in C_s symmetry, but none of them is a true transition state; they have two or three imaginary frequencies. Moreover, the energies of these high-order stationary points are higher than that of **16**. Thus, in the better mechanism (A), the H₂ molecule approaches the ethyl cation in C_s symmetry, leading to **3**. While H₂ approaches one of the carbons, the bridging hydrogen simultaneously moves to the other carbon. This process involves a barrier of 2.9 kcal/mol. The corresponding barrier for dissociation of C₂H₇⁺ (**3**) into C₂H₅⁺ (**8**) + H₂ is 9.1 kcal/mol (Table 2).

Continuing interest in gas-phase proton-transfer reactions has led to the definition of two related quantities, proton affinity and gas-phase basicity.³⁵ The proton affinity gives a quantitative

(35) Dixon, D. A.; Lias, S. G. In *Molecular Structure and Energetics*; Liebmann, J. F., Greenberg, A., Eds.; VCH Publishers, Inc.: Weinheim, Germany, 1987; Vol. 2, Chapter 7.

Table 8. Experimental and Theoretical Heats of Formation of Cationic Species (in kcal/mol at 298 K)

| researchers | year | CH ₃ ⁺ | C ₂ H ₅ ⁺ | CH ₃ ⁺ | C ₂ H ₇ ⁺ | ref |
|-------------------|------|------------------------------|--------------------------------------------|------------------------------|--------------------------------------------|-----|
| Experimental | | | | | | |
| Lossing et al. | 1970 | 261 | 219 | | | 41 |
| Franklin et al. | 1972 | | | 222.1 | 218.8 | 42 |
| Kebarle et al. | 1976 | | | 221.1 | 215 | 8 |
| | | | | | 207.2 | 8 |
| McCulloh et al. | 1976 | 262.7 ^a | | | | 43 |
| Rosenstock et al. | 1977 | 262 ^a | 219 | | | 44 |
| Houle et al. | 1979 | 261.8 ± 0.5 | 219.2 ± 1.1 | | | 45 |
| Baer | 1980 | | 218.2 ± 1.0 ^a | | | 30 |
| | | | 215.3 ± 1.0 | | | 30 |
| Bohme et al. | 1980 | | | 218.8 ± 2.1 | | 33 |
| Bohme et al. | 1981 | | 216.6 ± 1.7 | | 204.8 | 31 |
| Traeger et al. | 1981 | 261.3 ± 0.4 | 216.0 ± 0.5 | | | 29 |
| Rosenstock et al. | 1982 | | 215.9 | | | 32 |
| Lias et al. | 1984 | | 215.6 | 216.0 | 202.0 | 28 |
| | | | | 217.5 | | 28 |
| Anicich et al. | 1984 | 260.5 | | | | 46 |
| Theoretical | | | | | | |
| Moran et al. | 1985 | 260.4 | | | | 47 |
| Pople et al. | 1987 | 261.6 | | 223.0 | | 34 |

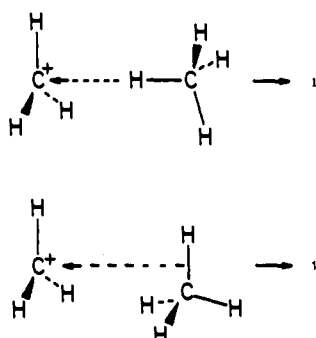
^a ΔH_f at 0 K.

Figure 5. Two possible pathways for addition of CH₄ to CH₃⁺. (a, top) The CH₃⁺ attacks CH₄ "end-on", initially along a C_{3v} symmetry pathway. A hydrogen atom of CH₄ acts as a σ-donor to the vacant p-orbital of the methyl cation. (b, bottom) CH₃⁺ attacks "side-on" with a C–H bond of CH₄ acting as a σ-donor. Both pathways lead to the C₂ symmetry structure 2.

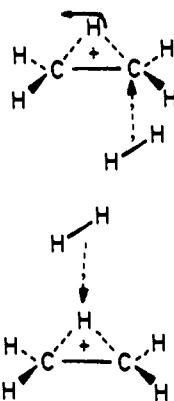


Figure 6. Two possible pathways for addition of H₂ to the ethyl cation. (a, top) The H₂ adds to C₂H₅⁺ at the backside. (b, bottom) H₂ attacks C₂H₅⁺ from above. Both mechanisms are concerted. While H₂ attacks one of the carbons, the bridging H moves to the other. This leads to the C₂ structure 3.

measure of the intrinsic basicity of a chemical compound^{33,36} and is defined as the negative of the standard enthalpy change of the reaction between a base and a proton to give an acidic species.^{35,37} For methane and ethane, the reactions defining the proton affinities are given in eqs 7a and 7b.³² Combining these equations gives the relative proton affinity of ethane versus methane (eq 8).

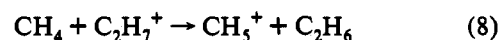
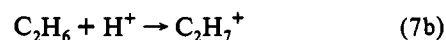
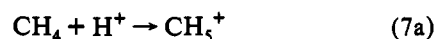


Table 9 summarizes the reported values for proton affinities (PAs) of methane and ethane and the results of the present study. The experimental values diverge considerably, not only due to the operationally different experiments but also due to the use of several standard reference scales. As shown in Table 8, the experimental heats of formation (on which the absolute PA values are based) of the cationic species vary considerably. The most recent determinations^{38,39} of the PA of methane give values between 130 and 131.6 kcal/mol (Table 9). For ethane there are two ranges of values, corresponding to the two protonated ethane isomers. The experimental PA of the more stable species was found to be between 137 ± 27^c and 146.9⁴⁰ kcal/mol; the PAs range from 131⁸ to 133 kcal/mol for the other species (Table 9). Although the absolute experimental estimates vary considerably, the PA difference between methane and ethane (to give the more stable C₂H₇⁺, 1) as determined in each individual investigation is rather constant, about 12 kcal/mol.^{8,28,31,33,40} This agrees with our computed results, corrected to 298 K (also given in Table 9). We calculate a PA of 130.0 kcal/mol for methane; for ethane the two values are 142.5 and 138.1 kcal/mol, leading to the C–C (1) and C–H (3) protonated ethane forms, respectively. The corresponding differences between the PAs of ethane and of methane, given by the standard enthalpy change of reaction 8, are 12.5 and 8.1 kcal/mol (Table 9). These differences as well as the individual PAs are in good agreement with previous theoretical results.^{15b,34}

(38) Adams, N. G.; Smith, D.; Tichy, M.; Javahery, G.; Twiddy, N. D.; Ferguson, E. E. *J. Chem. Phys.* **1989**, *91*, 4037–4042.

(39) Lias, S. G.; Bartness, J. E.; Liebmann, J. F.; Holmes, J. L.; Levin, R. D.; Mallard, W. G. *J. Phys. Chem. Ref. Data* **1988**, *17*, Suppl. 1.

(40) McMahon, T. B.; Kebarle, P. *J. Am. Chem. Soc.* **1985**, *107*, 2612–2617.

(41) Lossing, F. P.; Semeluk, G. P. *Can. J. Chem.* **1970**, *48*, 955–965.

(42) Chong, S.-L.; Franklin, J. L. *J. Am. Chem. Soc.* **1972**, *94*, 6347–6351.

(43) McCulloh, K. E.; Dibeler, V. H. *J. Chem. Phys.* **1976**, *64*, 4445–4450.

(44) Rosenstock, H. M.; Draxl, K.; Steiner, B. W.; Herron, J. T. *J. Phys. Chem. Ref. Data* **1977**, *6*, Suppl. 1.

(45) Houle, F. A.; Beauchamp, J. L. *J. Am. Chem. Soc.* **1979**, *101*, 4067–4074.

(46) Anicich, V. H.; Blake, G. A.; Kim, J. K.; McEwan, M. J.; Huntress, W. T., Jr. *J. Phys. Chem.* **1984**, *88*, 4608–4617.

(47) Shields, G. C.; Moran, T. F. *J. Phys. Chem.* **1985**, *89*, 4027–4031.

(36) Aue, D. H.; Bowers, M. T. In *Gas-Phase Ion Chemistry*; Bowers, M. T., Ed.; Academic Press: New York, 1979; Vol. 2.

(37) DeFrees, D. J.; McLean, A. D. *J. Comput. Chem.* **1986**, *7*, 321–333.

Table 9. Experimental and Theoretical Proton Affinities (PA) of Methane and Ethane (in kcal/mol at 298 K)

| researchers | year | PA(CH ₄) | PA(C ₂ H ₆) | PA(C ₂ H ₆) - PA(CH ₄) | ref |
|-------------------|------|----------------------|------------------------------------|-----------------------------------------------------------|--------------|
| Experimental | | | | | |
| Franklin et al. | 1972 | | 127.1 | | 42 |
| Bohme et al. | 1975 | | 140.4 | | ^a |
| Kebarle et al. | 1975 | | 137.4 ± 2 | | 7c |
| Kebarle et al. | 1976 | 127 | 131.8 | 4.8 | 8 |
| | | | 139.6 | 12.6 | 8 |
| Bohme et al. | 1980 | 130.5 ± 2 | | | 33 |
| Bohme et al. | 1981 | | 142.1 ± 1.2 | | 31 |
| Kebarle et al. | 1982 | 130 | 133 | 3 | ^b |
| | | | 141, 142 | 11, 12 | ^b |
| Lias et al. | 1984 | 132.0 | 143.6 | 11.6 | 28 |
| Kebarle et al. | 1985 | 134.7 | 146.9 | 12.2 | 40 |
| Lias et al. | 1988 | 131.6 | | | 39 |
| Adams et al. | 1989 | 130.0 | | | 38 |
| Theoretical | | | | | |
| Yamabe et al. | 1984 | 127.7 | 135.6 | 7.9 | 15b |
| | | | 139.7 | 12.0 | 15b |
| Dixon et al. | 1987 | 128.5 | | | 30 |
| Pople et al. | 1987 | 128.4 | | | 34 |
| Kutzelnigg et al. | 1990 | 130.5 | | | 14a |
| this work | | 130.0 | 142.5 (1) | 12.5 (1) | |
| | | | 138.1 (3) | 8.1 (3) | |

^a Bohme, D. K. In *Interactions between Ions and Molecules*; Ausloos, P., Ed.; Plenum Press: New York, 1975; p 489. ^b Hiraoka, K.; Kebarle, P. *Radiat. Phys. Chem.* **1982**, *20*, 41-49.

Conclusions

Our analysis of the C₂H₇⁺ potential energy surface reveals three minima, the C-C protonated structure **1** and the C-H protonated forms **2** and **3**. Only **1** and **2** have been considered before, but we find **3** to be 2.1 kcal/mol more stable than **2**. However, **2** and **3** are very similar and have a low conversion barrier for **2** into **3** (0.1 kcal/mol), so that only **1** and **3** should be observable experimentally; **3** is less stable than **1** by 4.4 kcal/mol. The methyl cation addition to methane or the reverse process, loss of CH₃⁺ from C₂H₇⁺, is interpreted in terms of a direct interaction between the methyl carbon and a C-H bond of methane leading to **1**. The latter rearranges into **3** with a barrier of 7.2 kcal/mol. Structure **3** can lose H₂ by 1,1-elimination. While the reaction of methane with the methyl cation does not require an activation energy, the H₂ elimination from C₂H₇⁺ (**3**) requires a barrier of 9.1 kcal/mol. The reverse addition reaction is calculated to involve a barrier of 2.9 kcal/mol. The barrier for conversion of **1** into **3** (7.2 kcal/mol) is calculated to be lower than the barrier for dissociation into C₂H₅⁺ + H₂ (13.6 kcal/mol). Hence, under favorable experimental circumstances, it is possible to observe deuterium scrambling when starting with labeled CH₃⁺ and CH₄.

The vibrational spectrum of **1** is characterized by the C-H stretching vibrations of the symmetrical bridging proton. As in other H-bridged species, these vibrations occur between 1900 and 2200 cm⁻¹. Other C-H stretching modes computed for **1** agree with those deduced experimentally. Nevertheless, neither **2** nor **3** can explain the second set of experimental spectral data. In particular, the experimental 3964-cm⁻¹ H-H stretching mode indicates a relatively weak bond of the H₂ moiety to the C₂H₅⁺ ion. Complexes between H₂ and bridged C₂H₅⁺ (**8**) were located, but these are too weakly bound to be candidates for the second C₂H₇⁺ species detected experimentally.

The proton affinity of methane is calculated to be 130.0 kcal/mol. The two values for ethane are 142.5 kcal/mol, leading to the more stable C₂H₇⁺ species, and 138.1 kcal/mol, leading to the second species.

Acknowledgment. This work was supported at Erlangen by the Deutsche Forschungsgemeinschaft, the Fonds der Chemischen Industrie, the Volkswagen-Stiftung, and the Convex Computer Corporation; in Georgia by the U.S. Department of Energy; and in Calgary by the Natural Sciences and Engineering Research Council of Canada. J. W. de M. Carneiro thanks CNPq-Brazil for financial support and DAAD-Germany for a grant during his stay in Erlangen.